Solar system science with subarcsecond slit spectroscopy

R. Dekany[a], D. Banfield[b], B. R. Oppenheimer[c,**], A. Bouchez[c], M. Brown[c],
T. Hayward[b,*], B. Brandl[b], M. Troy[a], G. Brack[a], T. Trinh[a], F. Shi[a]

[a]Jet Propulsion Laboratory, California Institute of Technology, Pasadena, CA 91109

[b]Cornell University, Ithaca, NY 14853

[c]California Institute of Technology, Pasadena, CA 91125

ABSTRACT

During its first year of shared−risk observations, the PALAO/PHARO adaptive optics system has been employed to obtain near−infrared R ~ 1000 spectra of solar system targets at spectroscopic slit widths of 0.5 and 0.1 arcsec, and corresponding spatial resolution along the slit as fine as 0.08 arcsec. Phenomena undergoing initial investigation include condensate formation in the atmospheres of Neptune, and the Saturnian moon, Titan. We present the results of this AO spectroscopy campaign and discuss AO specific considerations in the reduction and interpretation of this data.

Keywords: Adaptive optics, slit spectroscopy, Neptune, Titan

1. INTRODUCTION

The Cornell PHARO near−infrared science camera[1], used in conjunction with the JPL PALAO adaptive optics system at Palomar Mountain, supported the 'shared−risk' science observations for 9 observing programs during the past year. The majority of these programs, approximately 67%, included the collection of R ~ 1000 infrared spectra using the grism spectrometer mode provided by PHARO. Early science results of several of these observations are now in preparation. We choose here to consider one particular subset of observation, namely narrow−slit spectroscopy of solar system objects, and point out both the benefits of adaptive optics for these science programs and the special concerns in the planning, acquisition, and analysis of high−spatial−resolution slit spectra.
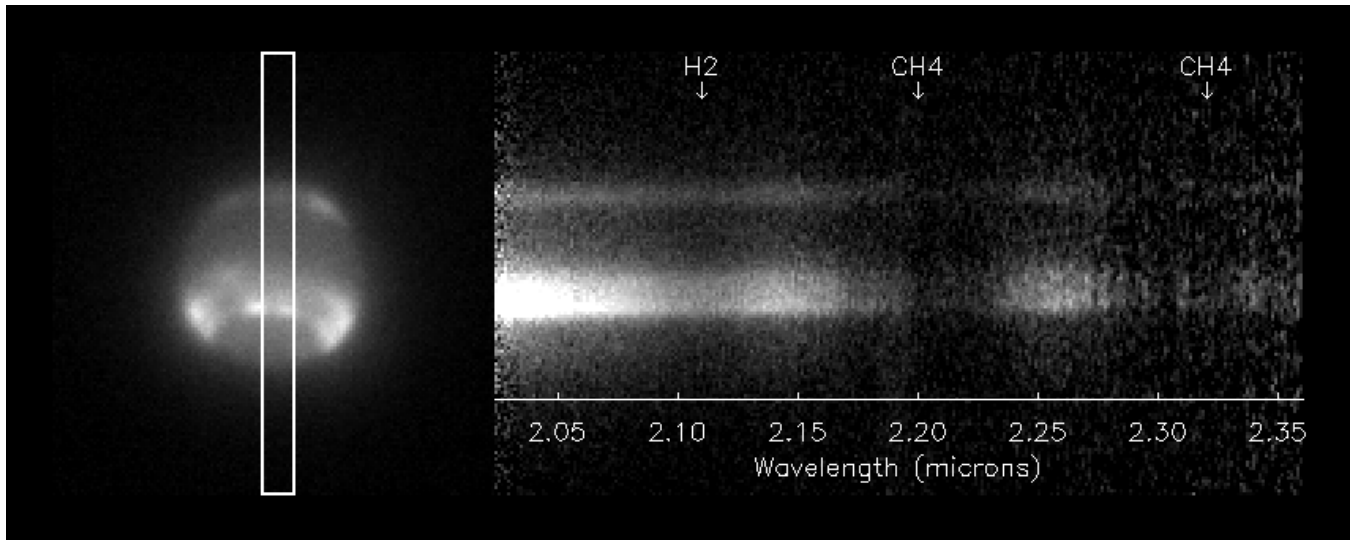
2. NEPTUNE

Spectroscopic observations of Neptune were obtained during the nights of Aug 26−29, 1999, with PHARO's spectroscopic slit aligned to yield various longitudinal cuts across the disk of the planet. Neptune itself was used as the guide object for the PALAO wavefront sensor. The finite size of the disk (~ 2.5 arcsec in diameter) did not seem to substantially degrade the PALAO performance, once suitable calibration of the wavefront sensor background level was performed. An example of the spectra obtained is shown in Figure 1. Between observations of Neptune, spectroscopic calibration data of the star HD190821 were obtained. While data analysis continues, we describe herein our approach to determining AO−enabled atmospheric science of Neptune.

The PHARO camera / spectrograph allows a spectral resolution of about 1000 in the K−band, within which Neptune's atmosphere has pressure−induced molecular hydrogen and strong rotation−vibration methane absorptions. By measuring the reflectivity of the planet across these molecular absorption bands, we can retrieve the vertical distribution of the scatterers reflecting the sunlight as a function of latitude for each of the longitudinal cuts obtained.

** Currently with University of California, Berkeley, CA 94620
* Currently with Gemini Observatory, Hilo, HI 96720

Figure 1. Neptune spectra (right) taken along a longitudinal slice of the AO–corrected disk (left).

Because methane condenses in the tropospheres of Neptune, its abundance as a function of altitude and position is not well known. Indeed, it is very likely dynamically controlled in the troposphere, and hence an interesting quantity to study. The hydrogen abundance is relatively well known, and its S(1) absorption feature around 2.11 μm can then be used to constrain the vertical sampling of the spectra. Using the hydrogen absorption wavelengths, we can retrieve the scatterer vertical distribution from each spectra. Then, methane abundances can be determined by comparing the reflectivities in the hydrogen absorption with those in the methane absorption. Vertical sensitivity extends from the optical depth unity level for the most opaque wavelength of hydrogen absorption down to a level where the integrated scatterer optical depth approaches unity. Below this, the single scattering analysis used in our retrieval approach breaks down.

For Neptune, this means pressures of roughly 100 mbar to perhaps 1 bar or more[2]. All of these results will be with significant latitudinal resolution on the planets and (eventually) for multiple longitudinal cuts. With the images already in hand, it is clear that there are discrete cloud features at certain latitudes and longitudes. The results of our detailed analysis when it is completed should clarify many interesting details of the circulation of Neptune's atmosphere.

To absolutely calibrate the spectra, a slightly modified version of the technique used by Banfield, et. al.[3] will be employed. This is to use calibrated narrow band filter images of the planets (calibrated via standard star observations), and then to compare given regions of the planet in these images with corresponding regions within the slit of the spectral images. By constraining the total flux in these regions in the narrow band images to equal that in the spectral images, integrated across the narrow band filter transmission curve, we can absolutely calibrate the spectral images.

For wavelengths at which Neptune has low reflectivity (I/F < 0.1), reflected photons will be overwhelmingly only singly scattered. Thus, the relation between scatterer distribution and reflectivity is linear and relatively easy to invert using least squares techniques. This is the approach outlined and used by Banfield, et. al.[3,4] to determine Jupiter's scatterer distribution. In those works, we used both hydrogen and methane absorption features to constrain the vertical profile of scatterers, since both gaseous species have well known abundances in the upper troposphere and lower stratosphere of Jupiter. However, for both Neptune, the methane abundance is not likely to be uniform vertically or horizontally because it condenses in the troposphere, nor is it very well known in a disk averaged sense.

We can still employ the known distribution of hydrogen and its known S(1) spectral absorption[5] near 2.11 μm to retrieve the vertical distribution of scatterers for Neptune. This would proceed nearly identically to the previous works for Jupiter, just with a smaller subset of wavelengths. Because the 2.11 μm hydrogen feature is not as opaque as the 2.3 μm methane feature, we will not be able to probe as high in the atmosphere of Neptune. Preliminary estimates of the highest weighting functions due to hydrogen absorption in the K band wavelengths have maxima at around 100 mbar[6]. For the Jupiter work, we were able to sense up to about 20 mbar. The deepest that we can sense is determined by the fact that we can only easily analyze singly scattered photons. By going to the wings of an absorption feature, we can sense deeper and deeper, until the

integrated optical depth becomes ~ 1 and reflected photons are likely to be multiply scattered. For Jupiter, this meant that we could sense to about 400 mbar (where the upper tropospheric haze becomes significantly more dense), while for Neptune, we may be able to sense to 1 bar or more[2, 7].

We can extend the analysis approach to also yield the methane abundance as a function of altitude much as it yields the scatterer abundance already. Conceptually, the same scatterers which were constrained using the spectra in the hydrogen absorption feature are also causing the reflectivity in the methane absorption feature wavelengths. The appropriate methane absorption coefficients are very poorly known in this wavelength region, but we have made significant recent progress in understanding these absorption coefficients using the GEISA database. In this case, we can use the (now known) scatterer distribution to determine the absorbing gas distribution over the same vertical extent as the scatterers are known.

We also intend to mine the results for insight into the dynamics and general circulations of the planets. Latitudinal differences in tropospheric scatterer density as a function of altitude are indicative of vertical motions in the atmosphere. A good example of this is the elevated tropospheric cloud seen around Jupiter's equator. These clouds may be indicative of a Hadley cell type circulation occurring there[3]. If similar structures are identified on Neptune, the possibility exists of confirming or refuting hypothesized atmospheric circulations of these planets[8]. The latitudinal distribution of stratospheric scatterers on Neptune can be used to infer their source regions (polar magnetospheric effects, or solar−input controlled photochemistry), and the meridional spreading they experience compared to their fallout rates (indicated by their latitudinal homogeneity or lack thereof). As with the scatterer abundance, the vertical, latitudinal and longitudinal variations of methane abundance are also indicative of atmospheric motions and condensations. The general circulation should influence the tropospheric meridional−vertical cross section of methane mixing ratio. Finally, if we identify latitudinal and/or longitudinal differences in Neptune's stratospheric methane abundance, it may be indicative of convective penetration events thought to be responsible for the possible stratospheric methane mixing ratio enhancement over cold trap amounts on Neptune.
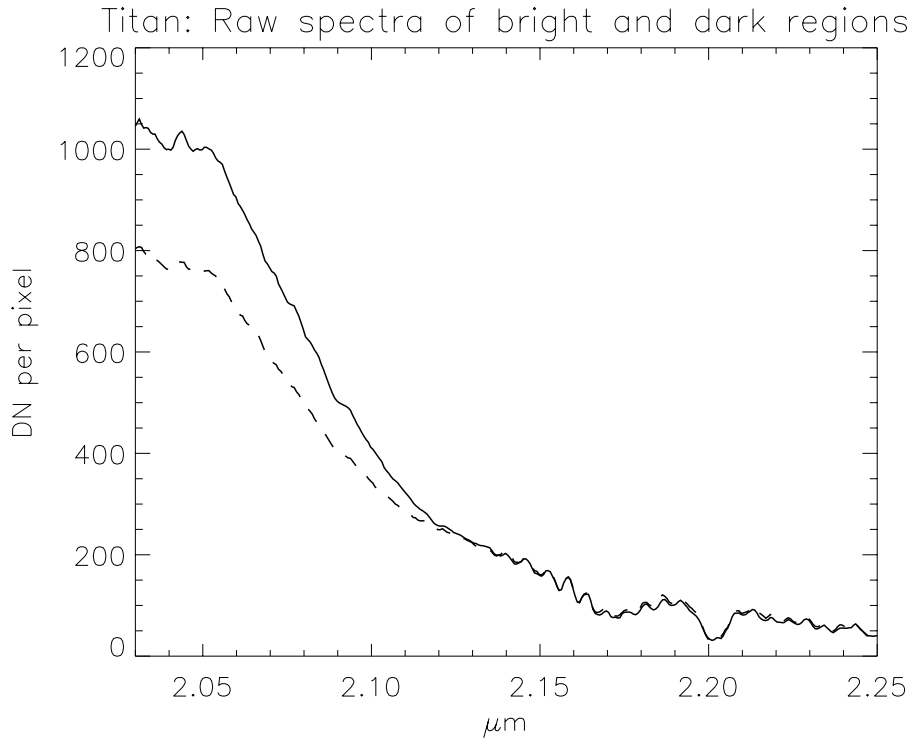

3. TITAN

The ability to acquire diffraction−limited, spatially resolved spectra of extended objects is one of the great promises of adaptive optics systems on large−aperture telescopes. Titan is an exciting first target for such observations. Voyager's cameras were unable to detect Titan's surface through its thick, hazy atmosphere but radio occultation and mid−infrared spectra suggested that Titan might experience the methane analogue of the Earth's hydrologic cycle, with methane clouds, rain, and perhaps hydrocarbon seas[9]. Recent high−resolution Hubble Space Telescope[10] and ground−based[11] imaging in the near−infrared has revealed what appear to be permanent surface features, though their compositional cause is so far unclear. Furthermore, haze distribution, possible tropospheric clouds, and surface albedo cannot be disentangled in these broad−band images.

Spatially resolved spectra of Titan taken with the Palomar AO system will allow us to isolate the contributions of the stratospheric haze, tropospheric clouds, and surface albedo in every spatial resolution element. In 3 hours of observation on 26 September 1999, we twice scanned the 0.1" wide PHARO spectrograph slit across Titan's disk, acquiring K band spectra at ~20 distinct locations on Titan's leading hemisphere. Between the atmosphere's saturated methane absorption bands, Titan's surface is detected, while wavelengths deep in the methane bands are sensitive only to the stratospheric haze distribution. A sample K−band spectrum, taken comparing two pixels of Titan's disk, one in the bright feature apparent on Titan's leading hemisphere, and the other north of this feature, is shown in Figure 2. Assuming only that the haze is longitudinally symmetric, we can model the spectra to determine the distribution of haze with latitude and height, detect the presence of any optically thick tropospheric methane clouds, and determine the surface albedo at every location. Initial results indicate that the haze optical depth decreases monotonically from the south pole (currently in mid−summer) to the north, and that we have detected tropospheric clouds near the south pole.

4. SPECTROSCOPIC OBSERVATION AND REDUCTION ISSUES

One of the most important applications of adaptive optics is spectroscopy. In principal adaptive optics permits one to make higher resolution spectra of objects in less time, because the light of the object is concentrated into a smaller point spread function, with enhanced peak brightness. Thus a smaller slit can be used. In our work with PALAO and PHARO we have attempted a variety of different spectroscopic observations, including separated spectra of close stellar

Figure 2. Sample raw K–band, R ~ 1000, spectra for two positions on Titan's leading hemisphere. The upper curve is taken from the higher albedo region near the center of the leading hemisphere, while the lower curve is taken from a lower albedo region.

companions and high spatial resolution spectroscopy of solar system objects. Several difficulties arise with such observations.

The most important stumbling block to this sort of work is the issue of dynamic range and contamination of spectra by other sources in or near the spectrograph's slit. In the case of separated spectra of close binary point sources, dynamic range overwhelms all other problems. The most astrophysically interesting objects to study in this case are systems in which a bright star is orbited by a very low–mass companion. We have found that the remaining light in the halo of the bright star's point spread function can be comparable to the light from the companion when the dynamic range between the star and the companion is greater than 5 magnitudes (in accord with Bloemhof et al. this volume who found that the peak halo brightness is nearly 1 to .1% of the core peak brightness). In this case, one must carefully choose the slit position angle in order to permit complete removal of the bright star's light. In practice it is much more useful to place the slit not at an angle perpendicular to the line connecting the companion and the star. By doing that, the spectrum of the star is maximized in the spatial axis on the position of the companion. Instead some oblique angle is preferable. This permits the extraction of the stellar spectrum completely separate from the companion's spectrum because the stellar signal will be maximized at some spatial location other than the companion's. In this way, one can fit the profile of the starlight in the spatial direction to determine the amount of contamination precisely. Then by extracting the star's spectrum one can subtract the appropriate amount from the companion spectrum.

For PALAO and PHARO this must be done with care. The slit position angle can be set with the Cassegrain Ring Rotation angle, but it can also be fine tuned with the tweaking controls in the PHARO user interface. While the fine tuning is not critical for the observations of the target object, one must be quite careful to ensure that the observations of the standard star be made at exactly the same slit angle with respect to the infrared array and at essentially the same row on the array. This is important for two reasons. First, the fringing inherent in the focal plane array is affected by the angle of the spectrum on the array, and, second, the slit is curved slightly, so that wavelength calibration is not necessarily the same at all pixel rows. While one can in principal correct for these problems in post processing, resampling the spectrum (to straighten it out or shift it in wavelength by a fraction of a pixel) introduces resampling noise. In the case of faint companions the introduction of any additional noise degrades the final signal substantially. Furthermore we have found

that the fringing problem is not particularly easy to overcome with resampling and shifting. It appears that the fringing may be a function of location on the array or in the shorter wavelength regime the fringes are not sampled by the pixels at the Nyquist frequency. This prohibits proper resampling.

ACKNOWLEDGEMENTS

REFERENCES

1. Hayward, T., Brandl, B., "Palomar High Angular Resolution Observer," in preparation.
2. Baines, K. H., and Bergstrahl, J. T., "The structure of the Uranian atmosphere: Constraints from the geometric albedo spectrum and H_2 and CH_4 line profiles," *Icarus*, **65**, 406−441, (1994).
3. Banfield, D., Conrath, B. J., Gierasch, P. J., Nicholson, P. D., Matthews, K., "Near−IR spectrophotometry of Jovian aerosols − meridional and vertical distributions," *Icarus*, **134**, 11−22, (1998).
4. Banfield, D., Gierasch, P. J., Squyres, S. W., Nicholson, P. D., Conrath, B. J., Matthews, K., "2μm spectrophotometry of Jovian stratospheric aerosols − scattering opacities, vertical distributions and wind speeds," *Icarus*, **121**, 389−410, (1996).
5. Borysow, A., "New model of collision−induced infrared−absorption spectra of H_2 −He pairs in the 2−2.5μm range at temperatures from 20 to 300K − an update," *Icarus*, **96**, 169−175, (1992).
6. Baines, K. H., Hammel, H. B., Rages, K. A., Romani, P. N., Samuelson, R. E., *Clouds and Hazes in the atmosphere of Neptune*, chapter in Neptune and Triton, D. P. Cruikshank, ed., U. Arizona Press, Tucson, (1995).
7. Baines, K., H., Hammel, H. B., "Clouds, hazes and the stratospheric methane abundance ratio in Neptune," *Icarus*, **109**, 20−39, (1994).
8. Conrath, B. J., Flasar, F. M., Gierasch, P. J., "Thermal structure and dynamics of Neptune's atmosphere from Voyager measurements," *J. Geophys. Res. Suppl.*, **96**, 18931−18939, (1991).
9. Lindal, G.F., Wood, G.E., Holtz, H.B., Sweetnam, D.N., Eshleman, V.R., and Tyler, G.L., Icarus, **53**, 348, (1983).
10. Smith, P.H., Lemmon, M.T., Lorentz, R.D., Sromovsky, L.A., Caldwell, J.J., and Allison, M.D., Icarus, **119**, 336, (1996).
11. Gibbard, S.G., Macintosh, B., Gavel, D., Max, C. E., de Pater, I., Ghez, A. M., Young, E.F., and McKay, C. P., Icarus, **139**, 189, (1999).